Determination of the Rate Constant of the $O + H_2 \rightarrow OH + H$ Reaction using Atomic Oxygen Resonance Fluorescence and the Air Afterglow Techniques

RICHARD N. DUBINSKY AND DONALD J. MCKENNEY[1]

Department of Chemistry, University of Windsor, Windsor, Ontario N9B 3P4

Received May 12, 1975

RICHARD N. DUBINSKY and DONALD J. MCKENNEY. Can. J. Chem. **53**, 3531 (1975).

Measurements of the rate of the reaction

[1] $$O(^3P) + H_2(^1\Sigma_g^+) \rightarrow OH(^2\Pi) + H(^2S_{1/2})$$

were made over the temperature range of 347 to 832 K and a pressure range of 140 to 739 N m^{-2}. Experiments were carried out using a discharge fast-flow system with a fixed observation port. O atoms, generated by the $N + NO \rightarrow N_2 + O$ reaction, were reacted with H_2 added downstream under pseudo first-order conditions ($[H_2] \gg [O]$). Relative O atom concentrations were determined using two independent methods: atomic resonance fluorescence at 130.6 nm and the air afterglow technique. The rate coefficients derived from our data can be expressed as $k_1 = (8.3 \pm 3.8) \times 10^{-12} \exp\{-36.0 \pm 2.0 \text{ kJ mol}^{-1}/RT\}$ cm^3 $molecule^{-1}$ s^{-1} (by resonance fluorescence), and $k_1 = (8.8 \pm 5.0) \times 10^{-12} \exp\{-34.9 \pm 2.0 \text{ kJ mol}^{-1}/RT\}$ cm^3 $molecule^{-1}$ s^{-1} (by air afterglow method). Comparisons are made with selected published results.

The Arrhenius plot of our data shows no evidence of curvature at low temperature.

RICHARD N. DUBINSKY et DONALD J. MCKENNEY. Can. J. Chem. **53**, 3531 (1975).

On a mesuré la vitesse de la réaction

[1] $$O(^3P) + H_2(^1\Sigma_g^+) \rightarrow OH(^2\Pi) + H(^2S_{1/2})$$

à des températures allant de 347 à 832 K et à des pressions de 140 à 739 N m^{-2}. On a effectué des expériences impliquant un système de décharge à flux rapide avec un point d'observation fixe. On a fait réagir les atomes d'oxygène, générés par la réaction $N + NO \rightarrow N_2 + O$, avec de l'hydrogène additionné en aval sous des conditions de réaction de pseudo premier ordre $[H_2] \gg [O]$. On a déterminé les concentrations relatives d'atomes d'oxygène en faisant appel à deux méthodes indépendantes: la fluorescence de résonance atomique à 130.6 nm et la technique de la lueur de l'air.

Les coefficients de vitesse dérives de nos données peuvent etre exprimés sous la forme $k_1 = (8.3 \pm 3.8) \times 10^{-12} \exp\{-36.0 \pm 2.0 \text{ kJ mol}^{-1}/RT\}$ cm^3 $molécule^{-1}$ s^{-1} (par fluorescence de résonance) et $k_1 = (8.8 \pm 5.0) \times 10^{-12} \exp\{-34.9 \pm 2.0 \text{ kJ mol}^{-1}/RT\}$ cm^3 $molécule^{-1}$ s^{-1} (par la méthode de la lueur d'air). On fait des comparaisons avec des valeurs publiées choisies.

Le diagramme d'Arrhénius de nos données ne montre pas de courbature à basse température.

[Traduit par le journal]

Many studies (1*a*) of the rate of the $O + H_2 \rightarrow OH + H$ reaction have been made. Data obtained in discharge flow systems at temperatures of 400–900 K now appear to be fairly consistent. The low temperature end, however, is less well defined with very few data for temperatures below 400 K. Westenberg and de Haas (2) using e.s.r. detection of O atoms obtained curvature of their Arrhenius plot at temperatures from about 420 to 357 K. They attributed this behavior to quantum mechanical tunnelling.

In this paper we wish to report a series of experiments designed to measure the rate of the title reaction over a wide temperature range extending to temperatures as low as possible in our apparatus (832–347 K) and over a very wide range of O/H_2 ratio. Two methods of atom detection were employed: resonance fluorescence of atomic oxygen at 130.6 nm (3) and the well-known air afterglow technique (4). Results are compared with published work and an Arrhenius expression for k_1 is recommended for temperatures up to ~830 K. Published results obtained at high temperature ($T > 900$ K) from separate shock tube, ignition limit studies, etc. (1*a*) are much less consistent, but rate constants are generally higher than that predicted by extrapolation of the linear Arrhenius plot obtained at

[1]To whom correspondence should be addressed.

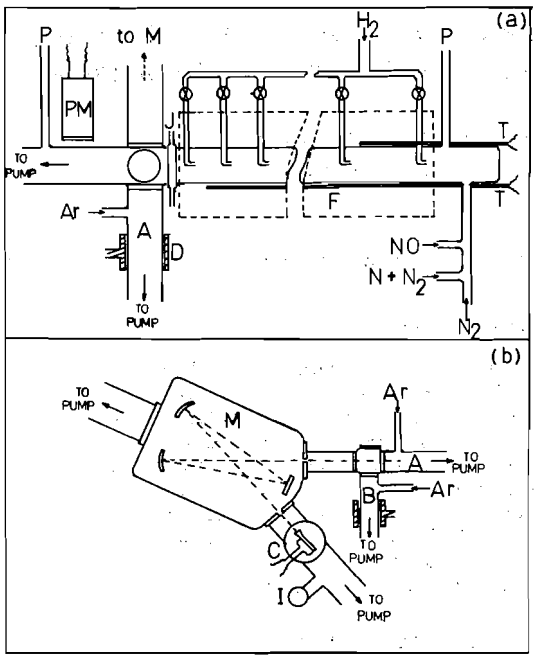

FIG. 1. (*a*) Schematic diagram of the quartz flow tube reactor. The first four jets closest to the observation cell are spaced 3 cm apart and the next five jets are 6 cm apart. Flow tube diameter is 2.50 cm i.d.; N + N_2, flow of N atoms in N_2 carrier from the discharge bypass; N_2, main carrier gas flow; P, connections to total pressure manometer; T, thermocouples (moveable); F, furnace; P M, photomultiplier tube; M, monochromator; J, cold water jacket; D, microwave discharge cavity; A, resonance fluorescence lamp. (*b*) Schematic top view of the observation cell and detector section. A and B, resonance fluorescence lamps; M, monochromator; C, Channeltron electron multiplier detector; I, ion gauge. Each section was separately pumped as described in the text.

low temperature. It has been suggested (5) that the O + H_2 reaction is therefore another example of a simple elementary process for which the rate coefficients at high temperature would be better represented on a curved Arrhenius plot. This point is discussed briefly.

Experimental

Flow System

A fast-flow discharge system was used for the production of $O(^3P)$ ground state atoms for reaction with ground state molecular hydrogen. Figure 1 shows a schematic diagram of the flow reactor and detection system. The $O(^3P)$ atoms were generated by the rapid reaction N + NO $\rightarrow$ N_2 + O, $k \simeq 3 \times 10^{-11}$ cm^3 molecule^{-1} s^{-1} (1*b*). The N atoms were formed by partial dissociation of molecular N_2 by passage through a 2.45 GHz microwave discharge (Microton 200) operated at 25–100 W power output. A discharge bypass arrangement as described by Clyne and Cruse (6) was used to obtain low [N]. Purified NO was added at known flows through a jet some 15 cm downstream of the discharge. The reactor flow tube was a 2.5 cm i.d. quartz tube provided with nine inlet jets spaced over a distance of 30 cm. Purified H_2 could be added through any of the jets or bypassed through an additional jet downstream of the observation ports.

For measurements at elevated temperatures a furnace was constructed around the reaction zone. The column was heated using Chromel heating element wire wound around the column in three sections, each of which was controlled by a variac auto transformer. Ceramic fiber held in place by asbestos board and covered with aluminum foil provided sufficient insulation. The temperature was measured at any point along the flow tube using two moveable chromel–alumel thermocouples located adjacent to the walls and on opposite sides of the flow tube. Simple adjustment of the variacs allowed temperature control to within ± 5 °C over the length of the reaction zone. A small water jacket surrounded the flow tube between the furnace and the observation port. The observation cell with its LiF windows was thus maintained at room temperature and protected from thermal shock.

The flow tube wall was coated with a mixture of CH_3SiCl_3 and $(CH_3)_2SiCl_2$ and baked at $\sim$400 K for several hours. This coating has been reported to inhibit atom removal on the wall (7).

Total pressure was measured at both ends of the flow tube, using a silicone oil manometer.

The downstream end of the flow tube led through a large bore (2.0 cm) stopcock to a liquid nitrogen-cooled high conductance trap to a Welch 500 l/min (model 1397) rotary pump.

Lamps and Detection Systems

The observation cell (Fig. 1*b*) was equipped with three polished LiF windows (Harshaw Manufacturing Co.). A fourth window of polished quartz which was positioned opposite Lamp B, (Fig. 1*b*), served to reduce scattered light entering the monochromator slit by multiple reflection. Lamps A and B were identical to each other and similar to that used by Bemand and Clyne (3). Cylinder argon dried by passage at low pressure through a liquid nitrogen-cooled trap packed with glass wool flowed through either lamp for excitation by means of a 2.45 GHz discharge operated at $\sim$25 W. Total pressure in the lamp was maintained at 1–2 $\times$ 10^2 N m^{-2} for a typical flow rate of $\sim$1 μmol s^{-1}. The conditions used were chosen to maximize the signal-to-noise ratio.

For those experiments in which relative [O] was measured from air afterglow intensities, the detector was an RCA 1P28 photomultiplier tube fitted with a Wratten No. 61 gelatin filter which transmits between 490.0–600.0 nm (maximum at 520.0 nm). The photomultiplier was fixed adjacent to the flow tube just below the observation cell. Signal currents were measured using a Keithley model 417 high speed picoammeter.

The detector system for the resonance fluorescence studies consisted of a McPherson monochromator (0.3 m, model 218) joined to the flow reactor by a simple tube collimator which directs emitted radiation to the entrance slit. The monochromator incorporated a 1200 line mm^{-1} MgF_2 coated diffraction grating (blazed at 500 nm). De-

tection was accomplished using a Bendix Channeltron electron multiplier operated at 2800 V d.c. (the power supply, Fluke, model 408B, specified line regulation of 0.001%). Signal pulses were amplified with a home-made preamplifier and Ortec timing filter amplifier (model 454). Counting rates were obtained after discrimination (Ortec integral discriminator, model 421) by either a rate meter (Ortec model 441) recorder system or a digital counter (Ortec model 775), coupled to a variable timer (Ortec model 719).

A pressure of $\sim 6.5 \times 10^{-5}$ N m^{-2} was maintained in the monochromator detector system by separate pumping (Fig. 1).

Reagents

Nitrogen (Liquid Carbonic) 99.996% stated purity was further purified by passage at ~ 101.3 kN m^{-2} pressure over divided copper (673 K), copper oxide powder (673 K), followed by a cold trap at 195 K. On the low pressure side of the flow-meter was another trap maintained at 77 K which contained silica gel on glass wool. Argon (Liquid Carbonic) was dried by passage at low pressure through a glass-wool packed cold trap (77 K). Hydrogen (Liquid Carbonic) was passed through a catalytic purifier (Deoxo-Engelhard Mfg.) and a silica gel glass wool trap (77 K). Nitric oxide (Matheson) was distilled repeatedly at 77–195 K under vacuum.

Procedure

The reaction was followed by monitoring the decay of relative [O] by either atomic resonance fluorescence or by the air afterglow method. In the former method resonance radiation emitted by the microwave-powered lamp, served to excite atomic resonance fluorescence of O(^{3}P) in the flow tube reactor. Measurements of the photon fluxes were made at λ 130.6 nm, corresponding to the transition O, 3s,$^3S_1$–2p^4,$^3P_0$. The air afterglow method involved the addition of a slight excess of NO beyond the nitrogen afterglow extinction point so that the greenish yellow emission from excited NO_2 could be readily measured. The emission intensity under the conditions employed in this work is directly proportional to [O] (4).

Kinetic Analysis

The removal of O atoms is considered with reference to the following processes:

[1] $$O + H_2 \rightarrow OH + H$$

[2] $$O + OH \rightarrow O_2 + H$$

[3] $$OH + H_2 \rightarrow H_2O + H$$

Assuming a steady-state concentration of OH the rate expression for O-atom consumption is

$$\frac{-d[O]}{dt} = k_1[O][H_2]\left(1 + \frac{1}{1 + \frac{k_3[H_2]}{k_2[O]}}\right)$$

$$= \alpha k_1[O][H_2]$$

where α corresponds to the term in parentheses. α, which must have values between 1 and 2, can be calculated for each run provided the ratio $[H_2]/[O]$ is known since k_2 and k_3 are both reasonably well established (8): $k_2 = (4.2 \pm 1.7) \times 10^{-11}$ cm^3 molecule^{-1} s^{-1} ($E = 0$), $k_3 = 3.8 \times 10^{-11}$ exp $\{-21.6$ kJ mol$^{-1}/RT\}$ cm^3 molecule^{-1} s^{-1}.

Most studies carried out in discharge flow systems have been studied under conditions such that only reactions 1 and 2 need be considered. In this work, however, the ratio $[H_2]_0/[O]_0$ was varied over a very wide range ($\sim$2000 to 40) partly because the resonance fluorescence work necessitated limiting [O] to values less than 2×10^{13} cm^{-3}. With very large $[H_2]_0/[O]_0$ ratios reaction 3 can be quite important relative to [2] for OH removal. Therefore, the contribution of reaction 3 was calculated for each run and the rate constant k_1 determined from plots of the equation

$$\log \{[O]_0/[O]\} = \frac{\alpha k_1}{2.303}[H_2]_0 t$$

A small correction ($\sim$5% maximum) was made for any pressure gradient along the length of the flow tube. Corrections for radial axial and back diffusion were found to be negligible.

Results

Heterogeneous Removal of H, OH, and O

A series of runs were carried out with the intention of obtaining k_1 by measuring the rate of production of H atoms. In this case Lyman-α resonance fluorescence at λ 121.6 nm was used to monitor relative [H] as a function of time. The data, which tended to show rather large scatter, indicated rapid loss at the wall. The H-atom fluorescence signal generally passed through a maximum with increasing reaction distance. Unfortunately, a quantitative comparison of H production to O loss was not possible. However, loss of H by heterogeneous processes is not expected to affect the kinetics of O decay (9).

If first-order OH removal on the wall was rapid enough, the apparent calculated value of k_1 may be too low by as much as a factor of two. This requires k_w^{OH} (rate coefficient for wall removal of OH) to be of the same magnitude or larger than $k_2[O]$. Thus, for $[O] = 10^{11}$–10^{13} cm^{-3}, k_w^{OH} would have to be greater than 10^2–10^3 s^{-1}. Recent estimates (10) of k_w^{OH} in similar systems have produced values of $\sim$10–100 s^{-1}. Although surface activity is often not compar-

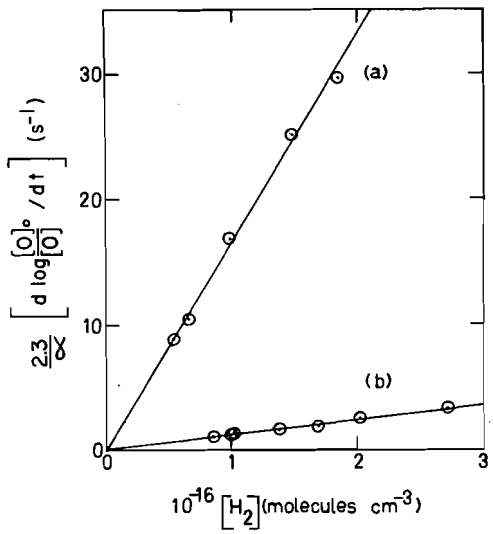

FIG. 2. Plot of $(2.3/\alpha)$[d log $\{[O]_0/[O]\}/dt$] *vs.* hydrogen concentration. (*a*) 508 K; by the resonance fluorescence technique. (*b*) 375 K; by the air afterglow method.

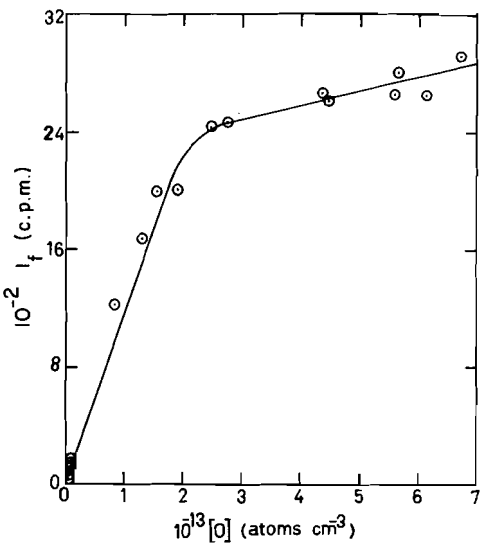

FIG. 3. Plot of fluorescence intensity (corrected for background) *vs.* oxygen atom concentration at λ 130.6 nm (unresolved) showing approximate linearity up to $\sim 2 \times 10^{13}$ cm^{-3}. (See ref. 3.)

able from one apparatus to another, the close agreement of our kinetic data (below) with those obtained by others suggests that heterogeneous removal of OH was not a serious problem in this work. Variation of $[O]_0$ over the range 10^{11}–10^{13} cm^{-3} produced no significant change in the value of k_1 calculated on the basis of negligible OH removal by heterogeneous processes.

Wall removal of O atoms does not interfere with the kinetic analysis provided that the removal is first-order and wall activity is not a function of added hydrogen (9). This assumption was verified by plots of [d log $[O]_0/[O]$)]/dt × $(2.3/\alpha)$ *vs.* $[H_2]$ (Fig. 2). Within experimental scatter, these were straight lines with zero intercept, confirming that [1] is strictly first order with respect to $[H_2]$.

k_1 by Resonance Fluorescence

Pseudo first-order conditions were used throughout with H_2 in great excess ($[H_2]_0/[O]_0$ ~2000–40) (see Table 1*a*). The oxygen triplet emission from the source was readily resolved and showed considerable self-reversal typical of such lamps (3). Peak ratios were 1:2:2 which is to be compared with the theoretical ratios of 1:3:5 for the O $^3S_1$–$^3P_0$ (λ 130.6 nm), O $^3S_1$–$^3P_1$ (λ 130.5 nm), and O $^3S_1$–$^3P_2$ (λ 130.2 nm) respectively. In the fluorescence mode, however, loss of radiation necessitated the use of large slit widths (typically 100 μm) on the monochromator preventing full resolution under most conditions. Nevertheless, a few calibration runs showed that the intensity of the peak centered at λ 130.6 nm was approximately a linear function of [O] up to $\sim 2 \times 10^{13}$ cm^{-3} (Fig. 3). This result is consistent with the very extensive work of Bemand and Clyne (3) who obtained data for each line of the O $^3S_1$–^3P_J multiplet. Initial O atom concentrations[2] were kept below 2×10^{13} cm^{-3} to ensure linearity of fluorescence signal with [O].

Figure 4*a* shows a typical plot of log $[O]_0/[O]$ *vs.* time obtained by this technique. Table 1*a* summarizes all data obtained from resonance fluorescence measurements corrected for background levels of scattered light (typically ~50 Hz). The relatively low concentrations of O atoms required by this technique and the slow reaction rate restricted our measurements to temperatures above 495 K. Figure 5 shows an Arrhenius plot of all the data and the results are summarized in Table 2 in the form of Arrhenius parameters derived from a weighted least mean

[2] $[O]_0$ for the three runs done at 832 K (Table 1*a*) were slightly greater than 2×10^{13} cm^{-3}. At this temperature however, calculation shows that the concentration of O is reduced to $< 2 \times 10^{13}$ cm^{-3} in $< 7 \times 10^{-3}$ s (corresponding to < 10 cm). Thus, the relative changes in [O] for the jets within 10 cm of the observation cell were in error and were therefore ignored in determining the slope.

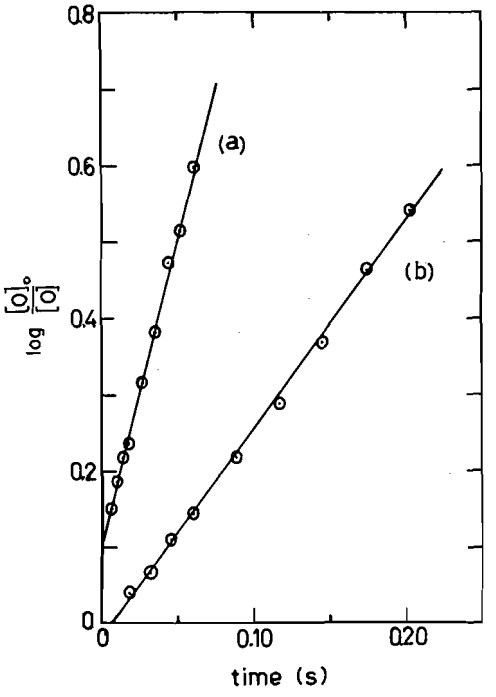

FIG. 4. Decay plots of relative [O]: (*a*) 508 K; resonance fluorescence technique, P_{tot} = 320 N m^{-2}, $[H_2]_0$ = 1.13 × 10^{16} molecules cm^{-3}, $[O]_0$ = 8.4 × 10^{12} atoms cm^{-3}; (*b*) 375 K; air afterglow technique. P_{tot} = 522 N m^{-2}, $[H_2]_0$ = 2.72 × 10^{16} molecules cm^{-3}, $[O]_0$ = 1.93 × 10^{14} atoms cm^{-3}. Zero of time scale differs from reaction time = 0.

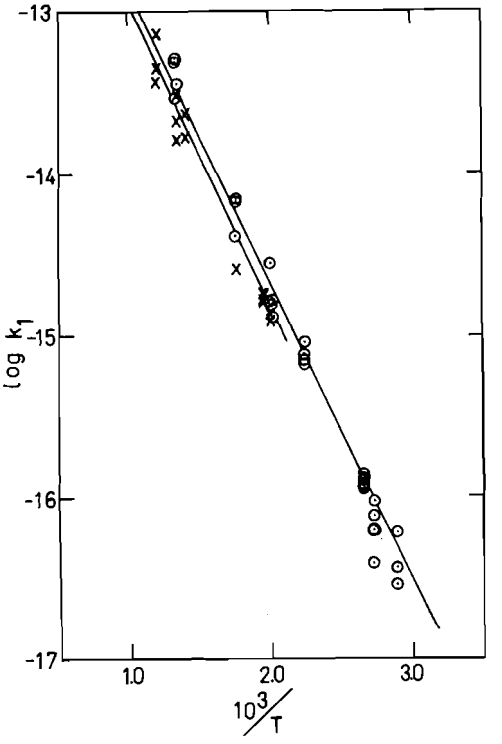

FIG. 5. Arrhenius plot of all data obtained in this work. ×, resonance fluorescence data; ○, air afterglow data.

squares analysis (see Appendix). Error limits quoted are 2σ (σ is the standard deviation). The statistical treatment applied to our resonance fluorescence data yields a 'best' line which is ~25% lower than that derived from our air afterglow results over the range 495–832 K. However, within the rather large uncertainty limits cited, the Arrhenius frequency factor and activation energy determined by both techniques are in reasonable agreement. Results also agree with those of Clyne and Thrush (11) but are significantly lower than those determined using the e.s.r. technique by other workers (12–14).

k_1 by the Air Afterglow Method

Measurements by this technique were carried out over the temperature range of 347–742 K which well overlaps the range studied by resonance fluorescence. The minimum ratio $[H_2]/[O]$ was approximately 40. At the lowest temperature $[H_2]/[O] \sim 1000$ with $[H_2] \sim 4 \times 10^{16}$ cm^{-3} (corresponding to a mole fraction $\chi_{H_2} \sim 0.2$).

Figure 4*b* shows a typical decay plot obtained by the air afterglow technique and results are listed in Table 1*b*. No significant contribution to the total emission photocurrent by HNO was expected using the Wratten No. 61 filter. Results are plotted, along with results from the resonance fluorescence experiments on Fig. 5. It can be seen that all the results are fairly consistent within experimental scatter. The derived Arrhenius parameters are shown in Table 2.

For comparison Table 2 and Fig. 6 also show results from other studies. Over approximately the same temperature range, all rate coefficients are generally in good agreement, but the Arrhenius parameters obtained from the data of Balakhnin *et al.* (14) are considerably higher than all others.

Discussion

The existing data on the O + H_2 reaction have been reviewed several times in recent years (1*a*).

TABLE 1

(*a*) Resonance fluorescence results

T (K)	Total pressure (N m^{-2})	$[H_2]_0$ (10^{15} molecule cm^{-3})	$[O]_0$ (10^{12} atom cm^{-3})	$\frac{d \log ([O]_0/[O])}{dt}$ (s^{-1})	α	k (cm^3 molecule^{-1} s^{-1})
832	208	1.69	22	39.7	1.25	4.33×10^{-14}
	273	1.00	29	21.5	1.42	3.49×10^{-14}
	366	1.98	33	78.4	1.30	7.01×10^{-14}
						Av. $(4.94 \pm 1.84) \times 10^{-14}$
742	335	5.80	16	42.1	1.09	1.53×10^{-14}
	334	4.41	12	62.1	1.09	2.98×10^{-14}
						Av. $(2.26 \pm 1.03) \times 10^{-14}$
734	156	2.53	11	25.8	1.14	2.06×10^{-14}
714	259	0.97	5.8	7.95	1.20	1.57×10^{-14}
	263	1.58	5.8	17.4	1.14	2.22×10^{-14}
						Av. $(1.90 \pm 0.46) \times 10^{-14}$
570	411	5.68	18	7.49	1.25	2.43×10^{-15}
508	230	5.40	7.8	4.64	1.21	1.64 ± 10^{-15}
	307	6.52	6.4	5.23	1.15	1.61×10^{-15}
	320	9.94	7.4	8.17	1.12	1.69×10^{-15}
	479	14.9	11	12.2	1.12	1.68×10^{-15}
	572	18.6	10	14.0	1.09	1.59×10^{-15}
						Av. $(1.64 \pm 0.04) \times 10^{-15}$
498	182	4.89	4.9	3.2	1.17	1.29×10^{-15}
	314	8.55	17	5.47	1.29	1.14×10^{-15}
						Av. $(1.22 \pm 0.11) \times 10^{-15}$

(*b*) Air afterglow results

T (K)	Total pressure (N m^{-2})	$[H_2]_0$ (10^{15} molecule cm^{-3})	$[O]_0$ (10^{12} atom cm^{-3})	$\frac{d \log [O]_0/[O]}{dt}$ (s^{-1})	α	k (cm^3 molecule^{-1} s^{-1})
742	337	5.37	18.2	73.8	1.11	2.85×10^{-14}
	333	4.41	10.8	103	1.08	4.98×10^{-14}
	224	2.97	10.1	70.5	1.11	4.92×10^{-14}
						Av. $(4.25 \pm 1.21) \times 10^{-14}$
734	156	2.43	12.5	42.8	1.16	3.50×10^{-14}
570	145	2.01	18.1	8.77	1.49	6.74×10^{-15}
	140	1.94	17.5	8.55	1.49	6.81×10^{-15}
	410	5.68	25.7	12.9	1.32	3.96×10^{-15}
						Av. $(5.84 \pm 1.63) \times 10^{-14}$
498	181	4.90	4.9	6.85	1.17	2.75×10^{-15}
	314	8.55	24.2	7.92	1.37	1.56×10^{-15}
						Av. $(2.16 \pm 0.84) \times 10^{-15}$
495	197	4.58	7.21	3.14	1.25	1.26×10^{-15}
	197	4.58	9.6	4.08	1.31	1.57×10^{-15}
	197	4.58	8.9	3.98	1.29	1.55×10^{-15}
						Av. $(1.46 \pm 0.17) \times 10^{-15}$
446	405	5.20	124	3.81	1.90	8.88×10^{-16}
	427	5.56	25	2.49	1.63	6.33×10^{-16}
	328	4.30	29.8	2.12	1.72	6.60×10^{-16}
	398	8.38	89.1	4.97	1.80	7.59×10^{-16}
						Av. $(7.35 \pm 1.15) \times 10^{-16}$
375	164	8.50	27.1	0.82	1.78	1.25×10^{-16}
	203	10.5	35.7	1.09	1.79	1.34×10^{-16}
	266	13.8	52.9	1.33	1.81	1.23×10^{-16}
	322	16.8	67.9	1.47	1.82	1.11×10^{-16}
	348	9.95	69.2	1.04	1.89	1.27×10^{-16}
	389	20.3	108	2.04	1.86	1.24×10^{-16}
	522	27.2	150	2.71	1.86	1.23×10^{-16}
						Av. $(1.24 \pm 0.07) \times 10^{-16}$
362	427	10.9	120	0.52	1.94	6.11×10^{-17}
	427	10.9	120	0.63	1.94	7.40×10^{-17}
	468	14.8	344	1.17	1.96	9.29×10^{-17}
	437	8.69	151	0.28	1.96	3.79×10^{-17}
						Av. $(6.65 \pm 2.31) \times 10^{-17}$
347	368	16.3	21.1	0.71	1.72	5.83×10^{-17}
	655	29.2	37.9	0.76	1.72	3.48×10^{-17}
	739	41.1	39.9	0.83	1.66	2.80×10^{-17}
						Av. $(4.04 \pm 1.59) \times 10^{-17}$

TABLE 2. Arrhenius parameters for the reaction $O + H_2 \rightarrow OH + H$

Method	T (K)	$A \times 10^{11}$ (cm^3 molecule^{-1} s^{-1})	E (kJ mol^{-1})	Reference
Air afterglow	347–742	0.88 ± 0.50	34.9 ± 2.0	This work
Resonance fluorescence	495–832	0.83 ± 0.38	36.0 ± 2.0	This work
Air afterglow	409–733	1.8 ± 0.6	38.4 ± 1.6	11
Electron spin resonance	423–910	3.5 ± 2.0	41.1 ± 2.8	12
Electron spin resonance and mass spectrometry	373–478	2.3 ± 0.8	39.5 ± 1.2	13
Electron spin resonance	408–520	9.4 ± 3.8	43.2 ± 1.4	14
All low temperature data[a]	347–832	1.6 ± 0.8	38.0 ± 2.0	

[a]Low temperature values were derived from averages at each temperature from this work and from refs. 11–14. A weighted least mean squares analysis of the Arrhenius plot yielded parameters cited (Appendix). Error limits are 2σ.

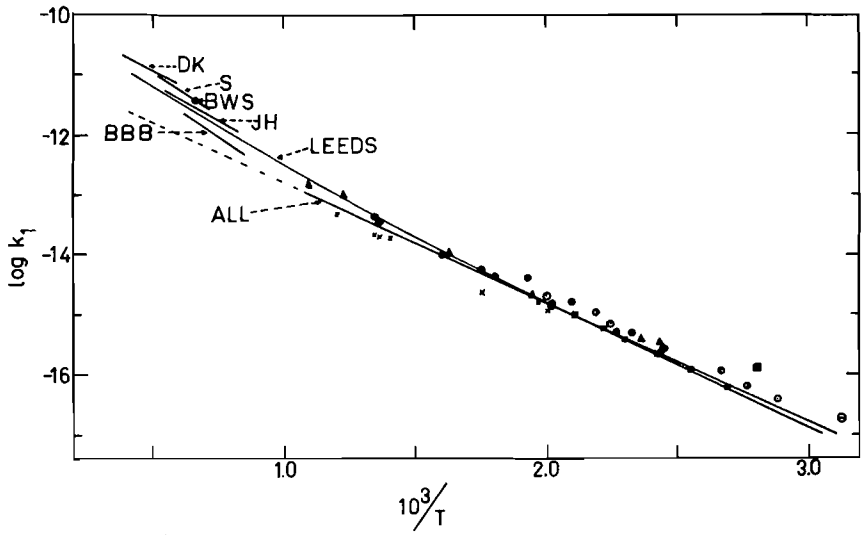

FIG. 6. Summary Arrhenius plot showing derived values of k_1, over the temperature range 320–~2600 K. DK, ref. 19; S, ref. 5; BWS, ref. 16; JH, ref. 17; BBB, ref. 18; LEEDS, ref. 1*a*; ALL, all low temperature data; △, ref. 12; ×, resonance fluorescence, this work; ○, air afterglow, this work; ◑, ref. 14; ●, ref. 11; ■, ref. 2; □, ref. 13; ⊖, ref. 15.

To our knowledge no new work at low temperature (<900 K) has appeared since the work of Balakhnin *et al.* in 1970 (14). Except for the few exceptions discussed in (1*a*) which for various reasons are not very reliable, the data reported is in fairly good agreement. In view of the variety of experimental techniques employed, considerable confidence can be placed in the results for the temperature range ~340–830 K.

Our data show no evidence of quantum mechanical tunnelling. We obtain a reasonably linear Arrhenius plot (Figs. 5 and 6) which (using the air afterglow technique) extrapolates to within ~11% of Campbell and Thrush's (15) value at 320 K. This linearity, however, is at variance with Westenberg and de Haas' results (2) which showed pronounced curvature at low temperature on their Arrhenius plot. The Westenberg and de Haas value at 357 K is approximately a factor of two higher than ours.

The last entry in Table 2 gives parameters derived from all low temperature data. It should be emphasized however that these values are not necessarily 'best' values. This is because a proper weighting of the data must take into account random and systematic errors in all data and this was not possible. On the other hand, data from all sources were statistically analyzed in the same way (Appendix). Therefore, the parameters derived from all low temperature data are probably the most reliable estimates which can be made at the present time. All the

low temperature (<900 K) results shown on Fig. 6, were selected as the most comprehensive and reliable, and nearly all values fall within about 50% of the 'all data' plot over the range 340–900 K. The discrepancy between our results and those of Westenberg and de Haas at low temperature is not readily explained. The excellent agreement of all workers over most of the temperature ranges studied probably rules out very serious systematic errors in flow calibrations etc. Assuming no large errors of this type, high values of k_1 would require enhancement of O decay, perhaps by heterogeneous processes involving H or OH.

Extrapolation of our results to the high temperature region (1000–2000 K) shows that a linear Arrhenius plot does not adequately describe the temperature dependence of this reaction over the extended temperature range. Figure 6 shows some of the more recent (post-1969) results acquired at high temperature in various shock tube and flame studies. The plot recommended by the Leeds group (Baulch *et al.* (1*a*) from an evaluation of selected low and high temperature results is also shown. The more recent data of Schott *et al.* would seem to indicate that the Baulch expression

$$k_1 = 3.0 \times 10^{-14} T \exp\{-37.2\ \text{kJ mol}^{-1}/RT\}\ \text{cm}^3\ \text{molecule}^{-1}\ \text{s}^{-1}$$

does not show quite enough curvature. Our low temperature results tend to bear out this conclusion.

There have been several other examples (20) of nonlinear Arrhenius behavior recently reported. Two different interpretations are usually made for this behavior. One, which has been applied in several cases (20), invokes transition state theory (t.s.t.). This was the approach taken by Schott *et al.* (5) to fit the low temperature results of Westenberg and de Haas (12) to their own high temperature data. In it the semiempirical bond-energy–bond-order (b.e.b.o.) method (21) which had earlier been applied to [1] by Mayer and Schieler (22) was combined with t.s.t. The computed values of k_1 fall along a smooth curve as expected, the curvature caused mainly by the changing contribution of a T^n term within the t.s.t. Gardiner *et al.* (23) have questioned the value of t.s.t. in this connection because of the large number of adjustable parameters required by the theory. Gardiner therefore prefers a second interpretation which in principle can be experimentally tested. This view suggests increasing participation of excited vibrational states of reactants with increasing temperature. The $O + H_2$ reaction presents an interesting test case. Because the energy separation between the first two vibrational levels in H_2 is very large (49.4 kJ (24)), the fraction of thermally produced vibrationally excited molecules ($H_2^{\ddagger}$) even at relatively high temperatures is quite small (*i.e.* $\sim 10^{-2}$ at 1500 K). Thus for reaction

[4] $$O + H_2^{\ddagger} \rightarrow OH + H$$

to contribute significantly to removal of O, an extremely large rate constant (at least equal to collision frequency) would be required if the high temperature results of Schott *et al.* (5) are to fit the low temperature data. We are now in the process of measuring k_4 in a newly designed apparatus by Lyman-α resonance fluorescence of H at λ 121.6 nm. Knowing k_1 the $O + H_2$ reaction can be used as a reliable calibration source for [H] (25) below 800 K.

We wish to thank the National Research Council of Canada for financial assistance in the form of an operating grant. We also wish to thank Dr. J. L. Hencher of this department for helpful discussions.

1. D. L. Baulch, D. D. Drysdale, D. G. Horne, and A. C. Lloyd. Evaluated kinetic data for high temperature reactions. Butterworths, London. (*a*) Vol. 1. 1972. p. 49; (*b*) Vol. 2. 1972. p. 171.
2. A. A. Westenberg and N. de Haas. J. Chem. Phys. **47**, 4241 (1967).
3. P. P. Bemand and M. A. A. Clyne. J. Chem. Soc. Faraday Trans. 2, **69**, 1643 (1973).
4. F. Kaufman. *In* Chemiluminescence and bioluminescence. *Edited by* M. J. Cormier, D. M. Hercules, and J. Lee. Plenum, New York. 1973. p. 83.
5. G. L. Schott, R. W. Getzinger, and W. A. Seitz. Int. J. Chem. Kinet. **6**, 921 (1974).
6. M. A. A. Clyne and H. W. Cruse. J. Chem. Soc. Faraday Trans. 2, **68**, 1281 (1972).
7. J. P. Wittke and R. H. Dicke. Phys. Rev. **103**, 620 (1956).
8. W. E. Wilson, Jr. J. Phys. Chem. Ref. Data, **1**, 535 (1972).
9. A. A. Westenberg and N. de Haas. J. Chem. Phys. **46**, 490 (1967).
10. M. A. A. Clyne and S. Down. J. Chem. Soc. Faraday Trans. 2, **70**, 253 (1974); J. G. Anderson, J. J. Margitan, and F. Kaufman. J. Chem. Phys. **60**, 3310 (1974); A. McKenzie, M. F. R. Mulcahy, and J. R. Steven. J. Chem. Phys. **59**, 3244 (1973).
11. M. A. A. Clyne and B. A. Thrush. Proc. R. Soc. London, Ser. A, **275**, 544 (1963).
12. A. A. Westenberg and N. de Haas. J. Chem. Phys. **50**, 2512 (1969).

13. K. HOYERMANN, H. Gg. WAGNER, and J. WOLFRUM. Ber. Bunsenges. Phys. Chem. **71**, 599 (1967).
14. V. P. BALAKHNIN, V. I. EGOROV, and V. N. KONDRATIEV. Dokl. Akad. Nauk. SSSR, **193**, 374 (1970).
15. I. M. CAMPBELL and B. A. THRUSH. Trans. Faraday Soc. **64**, 1265 (1968).
16. W. G. BROWNE, D. R. WHITE, and G. R. SMOOKLER. 12th Combust. Symp. The Combustion Institute, Pittsburgh, Pennsylvania. 1969. p. 557.
17. C. J. JACHIMOWSKI and W. M. HOUGHTON. Combust. Flame **15**, 125 (1970).
18. T. A. BRABBS, F. E. BELLES, and R. S. BROKAW. 13th Combust. Symp. The Combustion Institute, Pittsburgh, Pennsylvania. 1971. p. 129.
19. A. M. DEAN and G. B. KISTIAKOWSKI. J. Chem. Phys. **53**, 830 (1970).
20. A. A. WESTENBERG and N. DE HAAS. J. Chem. Phys. **58**, 4061 (1973); I. W. M. SMITH and R. ZELLNER. J. Chem. Soc. Faraday Trans. 2, **69**, 1617 (1973); W. C. GARDINER, JR., W. G. MALLARD, and J. H. OWEN. J. Chem. Phys. **60**, 2290 (1974); T. C. CLARK and J. E. DOVE. Can. J. Chem. **51**, 2147 (1973).
21. H. S. JOHNSTON. Gas phase reaction rate theory. Ronald Press Co., New York. 1966. p. 209.
22. S. W. MAYER and L. SCHIELER. J. Phys. Chem. **72**, 236 (1968); **72**, 2628 (1968).
23. W. C. GARDINER, JR., W. G. MALLARD, M. MCFARLAND, K. MORINAGA, J. H. OWEN, W. T. RAWLINS, T. TAKEYAMA, and B. F. WALKER. 14th Combust. Symp. The Combustion Institute, Pittsburgh, Pennsylvania. 1973. p. 61.
24. T. E. SHARP. At. Data, **2**, 119 (1971).
25. P. P. BEMAND, M. A. A. CLYNE, P. B. MONKHOUSE, and R. T. WATSON. Symposium on Chemical Kinetics Data for the Lower and Upper Atmosphere, Warrenton, Virginia, September 1974.
26. R. J. CVETANOVIĆ, R. P. OVEREND, and G. PARASKEVOPOULOS. Proceedings of the symposium in chemical kinetics data for the lower and upper atmosphere. *Edited* by S. W. Benson. Wiley Interscience, New York. 1975. p. 249.

Appendix

Evaluation of Arrhenius parameters from the familiar logarithmic form of the Arrhenius equation is usually done using an unweighted least mean squares treatment. However it has recently been pointed out (26)[3] that because the treatment involves a change in variable form k to $\ln k$ the low temperature data are in fact more heavily weighted. In order to compensate for this a weighted least squares treatment (26) is required where the weighting factor, $w_i' = w_i k_i^2$, is k^2/σ_k^2. (w_i are the statistical weights of the points.) In the case of the O + H_2 reaction, the k^2 term clearly dominates; *e.g.* $(k_{832}/k_{347})^2 \sim 10^6$. Thus the high temperature points are very heavily weighted. The standard deviation, σ_k, which is a measure of the precision of each k determination can be estimated from a complete assessment of the propagation of random errors. We have carried out this procedure for several experimental situations (below). Expected random errors generally fell in the range 9–28% using reasonable limits on each variable. This is to be compared with the observed scatter of 3–45% (σ) in the resonance fluorescence results and 6–40% (σ) in the air afterglow results. Such large scatter may indicate other sources of random error *e.g.* fluctuations in discharges, etc., which cannot easily be taken into account. We therefore used σ values from experimentally observed deviations for the weighting factors to derive the parameters cited in Table 2. (In cases where insufficient data were available estimates roughly equal to average σ's were made.) In two cases (refs. 13 and 14) rate constants were extracted from Arrhenius plots in order to apply the weighted least squares treatment, and in these cases the standard deviation for each point was arbitrarily (and optimistically) taken as 10%. Reference 11 gives average k's and corresponding deviations at each temperature. They were used 'as is'.

It is instructive to examine the consequences of the weighting procedure in detail on a set of apparently consistent data. Consider the most recent results of Westenberg and de Haas (12). They report the Arrhenius expression $k_1 = 5.3 \times 10^{11} \exp\{-42.7 \text{ kJ mol}^{-1}/RT\} \text{ cm}^3 \text{ molecule}^{-1} \text{ s}^{-1}$ for the range 500–900 K. Including their point at 423 K we obtain $k_1 = 3.2 \times 10^{-11} \exp\{-40.2 \text{ kJ mol}^{-1}/RT\} \text{ cm}^3 \text{ molecule}^{-1} \text{ s}^{-1}$. Both of these expressions were obtained using the unweighted least squares analysis. Using the weighted treatment with a weighting factor of $w_i' = k^2$ (which assumes all w_i are equal) we obtain the result, $k_1 = 8 \pm 4 \times 10^{-12} \exp\{-30.0 \pm 3.8 \text{ kJ mol}^{-1}/RT\} \text{ cm}^3 \text{ molecule}^{-1} \text{ s}^{-1}$! In this case the low temperature (and incidentally more precise) points are virtually ignored by the weighting treatment. Now taking $w_i' = k^2/\sigma^2$ and using standard deviations calculated from their data for each temperature we obtain $k_1 = 3.5 \pm 2.0 \times 10^{-11} \exp\{-41.1 \pm 2.8 \text{ kJ mol}^{-1}/RT\} \text{ cm}^3 \text{ molecule}^{-1} \text{ s}^{-1}$ which is the value cited in Table 2. While this is probably the best expression that can be derived from these data, it is clearly obvious that if accurate

[3]We thank one of the referees for drawing our attention to ref. 26 and for helpful suggestions.

Arrhenius parameters are to be obtained normal statistical distributions of data over a wide range of temperature must be available.

Propagation of Errors

Following Cvetanović *et al.* (26), estimates of random errors were made using the propagation of errors equation,

$$\sigma_Q = \left\{\sum_i \left(\frac{\partial F}{\partial M_i}\sigma_i\right)^2\right\}^{1/2}$$

where Q is the quantity being determined in the experiment from measurements, M_i. Q is a function F of M_i, $Q = F(M_i)$. σ_i are the standard deviations of the uncorrelated separate measurements M_i.

In this work k_1 was determined from

$$k_1 = \frac{2.303 \log ([O]_0/[O])}{\alpha[H_2]_0 t} = \frac{2.303(\text{slope})}{\alpha[H_2]_0}$$

The ratio $[O]_0/[O]$ is equal to the ratio of emission intensities measured, in the case of resonance fluorescence, as the number of photons less background counted over a 1 min period. In the air afterglow case it is measured as a current on a picoammeter. The rated time base accuracy is $< \pm 0.1\%$ for the Ortec (Model 719) timer. Statistical error in count rate amounts to $(\text{c.p.m.})^{1/2}$ which usually was $\sim \pm 2\%$. Rated error in current measurement is ± 2–3%. Nonlinearity of the resonance fluorescence signal *vs.* [O] at high [O] would contribute to the overall error. However, this is not expected to be a very serious problem since [O] is decreased quite rapidly in moderate reaction times.[2] At $[O] < 1 \times 10^{13}$ atom cm^{-3} linearity has been demonstrated for the λ 130.6 nm line (3).

Rapid deterioration of the LiF windows and consequent reduction of detection sensitivity was a serious practical problem since replacement of windows was not easily accomplished. For low signals the statistical error and spurious noise levels are relatively greater, possibly as large as 3%. Error in slope includes the random errors mentioned and also the error in t (s). The time, t, is calculated from $t = xAp/\sum F\,RT$ where x is the distance which defines the reaction zone, and A is the cross-sectional area of the flow tube, p is the total pressure, $\sum F$ is the total flow rate, R is the gas constant, and T is temperature. The errors in x and A are negligible and systematic. The error in T amounts to $\sim$1–1.5% (± 5 K). Pressures can generally be measured to at least ± 0.1 cm. For total pressures of 133–1000 N m^{-2} ($\sim$1–10 cm oil) the error amounts to 10–1%. The largest error in $\sum F$ probably arises from random fluctuations in flow rates but the error in flow meter readings can be significant for small Δp. We conclude that the combined error in t is of the order of $\pm$5–15% which generates a combined error of $\sim \pm$5–20% in the slope.

$$[H_2]_0 = \frac{f_{H_2}}{\sum F}\frac{p}{RT}$$

and therefore is considered precise to same limits as t ($\pm$5–15%). The error in $[O]_0$ can be quite large and contributes to the error in α. $[O]_0$ is equal to [NO] at the end point of the N + NO titration. This was usually determined visually. In addition the relatively low flows of NO are difficult to determine. Since $[NO] = f_{NO}p/(\sum F)RT$, errors in p, $\sum F$, and T also contribute. Limits of $\pm 30\%$ are therefore assumed. This, however, is not a large contributor to the overall error in k, because α is not very sensitive to small changes in $[O]_0$.

Substitution of all these limits into the propagation of errors equation leads to error values of $\pm$9–28% in k.